Transpupillary Collagen Photocrosslinking for Targeted Modulation of Ocular Biomechanics

BG Gerberich[a], **BG Hannon**[b], **A Hejri**[c], **EJ Winger**[c], **E Schrader Echeverri**[a], **LM Nichols**[c], **HG Gersch**[a], **NA MacLeod**[a], **S Gupta**[d], **AT Read**[a], **MD Ritch**[a], **S Sridhar**[a], **MG Toothman**[a], **GS Gershon**[a], **SA Schwaner**[b], **G Sánchez-Rodríguez**[a], **V Goyal**[e], **AM Toporek**[a], **AJ Feola**[a,h], **HE Grossniklaus**[f,g], **MT Pardue**[a,h], **CR Ethier**[a,b], **MR Prausnitz**[a,c]

[a]Wallace H. Coulter Department of Biomedical Engineering, Georgia Institute of Technology and Emory University, Atlanta, Georgia

[b]George W. Woodruff School of Mechanical Engineering, Georgia Institute of Technology, Atlanta, Georgia

[c]School of Chemical and Biomolecular Engineering, Georgia Institute of Technology, Atlanta, Georgia

[d]Daniel Guggenheim School of Aerospace Engineering, Georgia Institute of Technology, Atlanta, Georgia

[e]School of Electrical and Computer Engineering, Georgia Institute of Technology, Atlanta, Georgia

[f]Winship Cancer Institute of Emory University, Atlanta Georgia

[g]Department of Pathology and Laboratory Medicine, Emory University, Atlanta, Georgia

[h]Center for Visual and Neurocognitive Rehabilitation, Atlanta VA Healthcare System, Decatur, GA

Abstract

The central vision-threatening event in glaucoma is dysfunction and loss of retinal ganglion cells (RGCs), thought to be promoted by local tissue deformations. Here, we sought to reduce tissue deformation near the optic nerve head by selectively stiffening the peripapillary sclera, i.e. the scleral region immediately adjacent to the optic nerve head. Previous scleral stiffening studies to treat glaucoma or myopia have used either pan-scleral stiffening (not regionally selective) or regionally selective stiffening with limited access to the posterior globe. We present a method for selectively stiffening the peripapillary sclera using a transpupillary annular light beam to activate methylene blue administered by retrobulbar injection. Unlike prior approaches to photocrosslinking in the eye, this approach avoids the damaging effects of ultraviolet light by employing red light. This targeted photocrosslinking approach successfully stiffened the peripapillary sclera at 6 weeks post-treatment, as measured by whole globe inflation testing. Specifically, strain was reduced by 47% when comparing treated vs. untreated sclera within the same eye (n=7, $p<0.05$) and by 54% when comparing the peripapillary sclera of treated vs. untreated eyes (n=7, $p<0.05$). Post-treatment characterization of RGCs (optic nerve axon counts/density, and grading), retinal function (electroretinography), and retinal histology revealed that photocrosslinking was associated with some ocular toxicity. We conclude that a transpupillary photocrosslinking approach enables selective scleral stiffening targeted to the peripapillary region that may be useful in future treatments of glaucoma.

Graphical Abstract
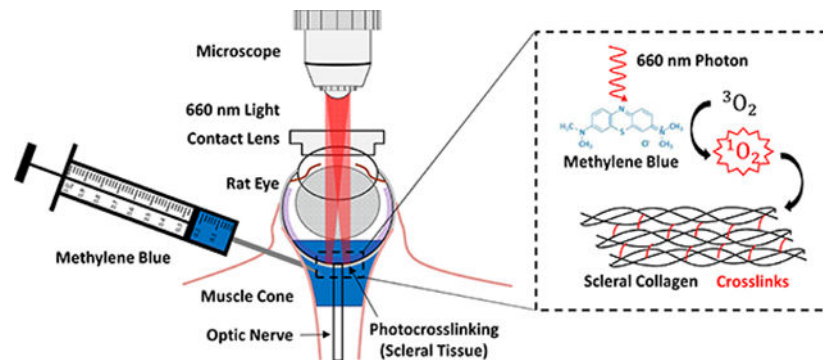
Keywords

Collagen Photocrosslinking; Scleral Stiffening; Ocular Biomechanics; Glaucoma; Myopia; Methylene Blue

2   Introduction

Glaucoma is the second leading cause of blindness in the world and affects approximately 70 million individuals worldwide [1,2]. Disease progression is associated with elevated intraocular pressure (IOP) and is characterized by cupping of the optic nerve head (ONH), posterior bowing of the lamina cribrosa, and damage to retinal ganglion cell (RGC) axons in the ONH [3]. While current glaucoma treatments primarily aim to lower IOP (which lessens the mechanical loading at the ONH), an alternative future strategy may be to mechanically

reinforce the peripapillary sclera (the scleral region immediately adjacent to the ONH). Such reinforcement may protect the ONH from pressure-induced injury [4,5].

Stiffening of the peripapillary sclera was previously shown to reduce mechanical strain in the lamina cribrosa of *ex vivo* porcine eyes [6,7]. However, an *in vivo* study found that whole-globe scleral stiffening worsened RGC axon loss in glaucomatous mice [8]. This result was unexpected considering the prior evidence of peripapillary scleral stiffening leading to reduction in lamina cribrosa strain and the belief that excessive mechanical strain damages RGCs [6]. An explanation for this result may be that whole-globe scleral stiffening reduces the overall compliance of the eye, causing IOP fluctuations to be larger in amplitude and hence more damaging [9]. We hypothesize such an effect may be overcome by targeted crosslinking of the peripapillary sclera, rather than whole globe stiffening.

Scleral stiffening has previously used either photomediated ("light") or non-photomediated ("dark") collagen crosslinking. Riboflavin crosslinking is a well-established procedure for treating the refractive disorder keratoconus, in which the photosensitizer, riboflavin, is applied topically to de-epithelialized corneas and exposed to ultraviolet A (UVA) light for 30 minutes [10,11]. The success of this method in keratoconus treatment has led to additional studies testing riboflavin's effects on scleral stiffening for myopia management [12,13]. However, riboflavin crosslinking has largely been limited to the anterior sclera due to the toxicity of UVA light at high doses and the difficulty of reaching posterior ocular tissues [14,15]. Recently, UVA light was delivered by an optic waveguide/optical fiber to equatorial rabbit sclera *in vivo* for targeted riboflavin photocrosslinking, generating interest in regionally-selective scleral stiffening [16].

In addition to photocrosslinking strategies, dark crosslinkers have been used for corneal and scleral stiffening [17,18]. Recently, we have shown the feasibility of *in vivo* scleral crosslinking with a single injection of the dark crosslinker, genipin [19]. However, small molecule dark crosslinkers typically stiffen the entire globe non-selectively, as they diffuse quickly through tissues and react with collagen on contact.

Methylene blue (MB) is a known type II (singlet oxygen-generating) photosensitizer and has found many medical uses since its discovery over a century ago, including as an anti-malarial, antidote for cyanide poisoning, and currently as a treatment for methemoglobinemia [20–24]. We chose MB for its efficient absorbance of red light (molar absorptivity, $\varepsilon = 73{,}300 \ \mathrm{M^{-1}cm^{-1}}$), high triplet quantum yield ($\phi_T = 0.52$), solubility, existing acceptance in clinical applications, and commercial availability [25,26]. Selection of a sensitizer absorbing in the phototherapeutic window (650–850 nm), where melanin and hemoglobin absorbances are relatively low, was an important criterion [27]. Furthermore, MB has been shown to increase collagen stability in rat tail tendon and to induce crosslinking of porcine pericardial tissue, suggesting it would perform well as a crosslinker in a collage-rich tissue such as the sclera [28–30].

Despite advances in both dark crosslinking and photocrosslinking approaches in the eye, none have achieved *in vivo* spatial selectivity on the millimeter scale necessary to selectively crosslink the peripapillary sclera while leaving the remainder of the globe unaffected. This

degree of spatial selectivity is needed to test the hypothesis that targeted crosslinking of the peripapillary sclera confers protection on RGCs in glaucomatous eyes. The goal of this study was to develop a method for selectively stiffening the peripapillary sclera, with the intent of achieving >40% reduction in mechanical strain in the peripapillary region, motivated by the *ex vivo* studies of Coudrillier et al. [6]. A photocrosslinking approach was chosen to achieve millimeter-scale targeted stiffening, and therefore considerations were made for using a light-activated crosslinking agent, delivery of that agent to the peripapillary sclera, and illumination of that agent with a transpupillary light beam. With our targeted approach, an annular light beam (wavelength 660 nm) with an outer and inner diameters of 2 mm and 1 mm, respectively, was projected onto the peripapillary sclera (which we define as the sclera within a circle of diameter 2 mm centered on the optic nerve) through the pupil. By establishing a method for targeted peripapillary photocrosslinking, future studies can test the viability of such a treatment as a neuroprotective strategy in glaucoma.

3 Materials and Methods

3.1 Overview of Individual Studies

Five studies were performed (summarized in Table 1) to assess: 1) transport of MB to the sclera after retrobulbar injection, 2) scleral stiffening in rats immediately after treatment, 3) scleral stiffening in rats 6 weeks after treatment, 4) retinal morphology of rats treated with MB and light, and 5) retinal morphology of rats treated with light only. In the study of scleral stiffening in rats 6 weeks after injection, multiple analyses were performed including: whole globe inflation testing (scleral stiffening), electroretinography (retinal function), and axon count (retinal/ON health).

3.2 Rats

Brown Norway retired male breeder rats (age 6–12 months) were obtained from Charles River Laboratories (Wilmington, MA). All procedures involving animals were approved by the Georgia Institute of Technology and Atlanta Veteran Affairs Healthcare System Institutional Animal Care and Use Committee (IACUC) and complied with the ARVO statement for the Use of Animals in Ophthalmic and Vision Research. Rats were housed and maintained by veterinary staff at the institute animal facility and were fed standard rodent diet (LabDiet 5001, Lab Supply, Fort Worth, Texas). Prior to any procedure, rats were allowed at least three days to become acclimated to the animal facility.

3.3 Anaesthesia and Eye Dilation

Rats were placed under anesthesia using a mixture of isoflurane gas (5%) and oxygen gas (95%) supplied through a nose cone fitted with a stereotaxic head positioner (Kopf Instruments, Tujunga, CA). A heating pad was placed under the rats to maintain body temperature throughout the procedure. After induction of anesthesia, 0.5% tetracaine eye drops (Tetracaine Hydrochloride Ophthalmic Solution, Amici Pharmaceuticals, Melville, New York) were applied topically to the eyes bilaterally. Excess fluid was gently wicked away from the surface of the eyes with a lab tissue, and 1% tropicamide dilating drops (Tropicamide Ophthalmic Solution, Henry Schein, Melville, New York) were applied bilaterally and allowed to take effect for approximately 10 min. Pupil dilation was confirmed

visually prior to each experiment to ensure sufficient visual access to the fundus. Anesthesia was maintained throughout the remaining duration of the procedure with an isoflurane/ oxygen flow rate of approximately 800 mL/min. At the conclusion of survival procedures, rats were allowed to recover from anesthesia on a heating pad, returned to their housing when ambulatory, and were monitored for any adverse effects of the procedure. For non-survival procedures, rats were euthanized by exposure to 100% CO_2.

3.4 Study 1: Confocal Microscopy/MB Distribution

Confocal microscopy was used to assess MB transport to the posterior sclera after retrobulbar injection. Injection solutions were prepared using 3 mM MB. Rats were randomly selected for each experiment and assigned to a diffusion time group of 30 min (n=5 animals), 20 min (n=3), or 10 min (n=5) from injection to death. Rats were anesthetized using isoflurane gas. Topical tropicamide (0.5%) followed by topical tetracaine (0.5%) were applied bilaterally, matching the experimental procedure used for photocrosslinking (though in this study, light was not applied). In this pilot study, a retrobulbar injection of 50 μl of MB solution was performed using a 3 mL insulin syringe in the OD eye, followed immediately by a retrobulbar injection of 50 μl of HBSS in the contralateral eye (OS). Five minutes prior to the total diffusion time assigned to each rat (10, 20, or 30 min), rats were exposed to CO_2 for euthanasia so as to ensure an accurate elapsed time for diffusion, since prior studies have shown that time from first breath of CO_2 to cessation of pulsatile blood flow (with the endpoint being death) is 5 min [31,32]. See Supplementary Information for tissue preparation and imaging procedures.

3.5 Studies 2 and 3: Day 0 and Six-Week Crosslinking Studies

To determine whether MB photocrosslinking resulted in targeted scleral stiffening, rats (n=7) were treated unilaterally with MB photocrosslinking and euthanized immediately post treatment for scleral stiffening measurements. Safety and duration of photocrosslinking were then assessed with rats (n=8) treated unilaterally with MB photocrosslinking and monitored for 6 weeks. Contralateral eyes received an equivalent volume of HBSS vehicle as a control. Electroretinograms were conducted prior to euthanizing the rats to assess retinal function. Whole globe inflation testing (see below) was performed on the eyes after euthanasia to investigate scleral stiffness. Optic nerves were collected immediately after euthanasia, fixed, and sectioned for axon counting and nerve grading.

3.5.1 Ocular Imaging and Photocrosslinking by Microscopy—We constructed an ophthalmic microscope (Figure 1) to enable simultaneous transpupillary fundus visualization and annular beam projection from an incoherent diode light source (M660L4, Thorlabs, Newton, NJ). The microscope rested on a three-axis manual micro-positioner, allowing for fine corrections in beam alignment, and was mounted with the objective and projected beam facing downwards toward a stereotaxic mount. Light intensity was adjusted using a variable power source/controller (T-cube LED Driver, LEDD1B, Thorlabs). An annular beam was formed from the diode source using an aperture, axicon lens, and microscope objective. A digital microscope camera was used to visualize the projected annular beam.

3.5.2 Photocrosslinking Materials—Methylene blue (MB; Apollo Scientific, Stockport, UK) in powder form was solubilized in Hank's balanced salt solution (HBSS) (Mediatech, Manassas, Virginia) resulting in a buffered solution with final MB concentration of 3 mM. HBSS buffer vehicle solution was chosen to neutralize the otherwise acidic nature of dissolved MB. The solution was heated to 100°C for 15 min to solubilize MB and subsequently allowed to cool prior to injection. Sterile, disposable syringes (300 μL) with 31 G needles (BD Insulin Syringes with BD Ultra-Fine™ needle, Becton, Dickinson and Company, Franklin Lakes, New Jersey) were filled with 100 μL of either HBSS or 3 mM MB solubilized in HBSS.

3.5.3 Photocrosslinking Procedure—After anesthesia induction and pupil dilation, a single 100 μL retrobulbar injection (inferior quadrant) was administered to each eye using forceps to gently proptose the eye. Our stereotaxic head mount equipped with a tooth bar (but no ear bars) allowed for rotation and elevation of the head as well as unobstructed access to the eyes. Syringes/needles were held in place for 10 s after injection to avoid reflux of fluid from the retrobulbar space. Hydrating eye lubricant (Puralube Vet Ointment, Dechra, Northwich, United Kingdom) was applied topically to the eye not receiving light to prevent dehydration during the photocrosslinking procedure.

Following retrobulbar injection, rats were positioned with the eye receiving light treatment facing upward and positioned in the optical path of the microscope. A contact lens designed for fundus imaging in rat eyes (OFA5.4, Ocular Instruments, Bellevue, Washington) was placed on the cornea and optically coupled to the surface with HBSS, allowing visualization of the fundus (Figure 1C).

A low intensity (< 0.1 mW) "guide" beam was used to locate the ONH through the microscope's camera. The beam projection was then aligned so that the optic nerve was positioned at the dark center of the annular beam (Figure 1D). After alignment, light intensity was adjusted to a power of 10 mW measured using an optical power meter (PM400, ThorLabs) and maintained for 30 min (Figure 1D).

The diode's nominal peak wavelength was 660 nm, i.e. visible red light. Annular beam dimensions were 1 mm inner diameter and 2 mm outer diameter, resulting in an intensity of approximately 425 mW/cm^2. Right and left eyes received alternating treatments from rat to rat to control for any variation due to orientation of the eyes.

3.6 Whole Globe Inflation Testing

To confirm the efficacy of scleral stiffening, scleral deformation as a function of intraocular pressure was measured *post mortem* using a digital image correlation (DIC) system (Dantec Dynamics, Skovlunde, Denmark) as previously described by Hannon et al. and others [6,18, 30]. Eyes were enucleated immediately after CO_2-induced euthanasia and excess orbital tissue was carefully removed with dissection microscissors to expose the sclera. After tissue removal, each eye was mounted with the optic nerve positioned upward under the downward-facing cameras on a custom pressurization apparatus by applying cyanoacrylate-based adhesive (Henkel, Düsseldorf, Germany) to the contact with the limbus. The cornea was excised, and the lens was removed to prevent any hinderance to subsequent

pressurization, leaving only the mounted scleral shell, which was filled with phosphate-buffered saline (PBS). The optic nerve was trimmed to leave approximately 1 mm protruding from the posterior scleral surface.

Graphite powder was applied to the posterior scleral surface to create a speckle pattern used by the DIC system cameras to track surface displacements. The mount with attached scleral shell was then secured with the anterior scleral surface in fluidic communication with a PBS pressure reservoir and in-line flow sensor (SLG64–0075, Sensirion, Staefa, Switzerland) used to monitor flow of PBS into the eye upon pressurization. An IOP of 3 mmHg was selected to represent the reference configuration when computing strains, as this was the minimum pressure for which the buckling of the scleral shell was reliably avoided. Area-weighted first principal Lagrange strains are reported in this study and were calculated from surface displacement measurements at 3, 10, 20, and 30 mmHg. Surface displacement data represented by individual "facets" (45×45 pixels) were tracked in the x, y, and z dimensions and compared to the 3 mmHg reference configuration for calculation of strain. Strain values reported in this study were calculated at 22 mmHg by extrapolation using a Fung model [34]. This method was chosen since using strain measurements at multiple pressures allowed for more accurate determination of the nonlinear strain-pressure relationship. We chose to report strains at 22 mmHg, since this is the mean IOP of awake, normotensive Brown Norway rats measured in our laboratory and others [19,35].

A walled, open-top chamber surrounding the eye was filled with PBS to prevent drying of the eye, and a layer of mineral oil was floated on top of the PBS to prevent evaporation of the PBS while maintaining a clear optical path between the sclera and cameras. The system was calibrated to account for refraction of PBS and mineral oil prior to testing. Care was taken to avoid excess light exposure during inflation testing to reduce the possibility of *post mortem* photocrosslinking. For detailed information on tissue preconditioning and DIC data analysis used, see Supplementary Information.

3.7 Electroretinography

Electroretinograms were measured using full-field electroretinography in a Ganzfeld dome (UTAS Big Shot, LKC Technologies, Gaithersburg, MD). After 30 min of dark adaptation, rats were anesthetized with a subcutaneous injection of ketamine/xylazine. Tetracaine (0.5%) and tropicamide (1%) were applied topically to locally anesthetize and dilate the eyes, respectively. Electrodes were placed subcutaneously in the cheek (reference) and tail (ground), and a gold loop electrode was placed in contact with the cornea (active). Scotopic recordings were taken in response to -3.0 to 2.1 log cd s m^{-2} flash stimuli of increasing luminance, followed by 10 min of light adaptation (1.5 log cd m^{-2}) and photopic recordings in response to 0.4 to 1.4 log cd s m^{-2} flash stimuli of increasing luminance. A flickering light stimulus (1.9 log cd s/m^2 at 6 Hz) was then used to isolate cone photoreceptor responses. Responses were differentially amplified (1 – 1500 Hz) using a signal-averaging electroretinography system (UTAS BigShot; LKC Technologies, Gaithersburg, MD). Representative voltage traces were reported for scotopic and photopic responses at the brightest flash stimuli (2.1 and 1.4 log cd s m^{-2}, respectively).

3.8 Optic Nerve Axon Counts

Axon counts were performed on the histological cross sections of optic nerves fixed in Sorensen's buffer containing glutaraldehyde (2.5%) and paraformaldehyde (PFA; 2%, EMS, Hatfield, PA) after enucleation. The nerves were subsequently embedded in epon-araldite plastic (Araldite 502/Embed 812, EMS, Hatfield, PA). Cross sections (0.5 μm thickness) were stained with toluidine blue and imaged on a Leica DM6 B microscope (Leica Microsystems, Buffalo Grove, IL) equipped with a X63 objective and X1.6 multiplier. Image tiles were collected and stitched together to create a montage of the entire optic nerve in cross section. Whole images of the optic nerve cross sections were then analyzed using a custom-designed deep learning-based computer algorithm (AxoNet) to automatically count axons deemed healthy [36]. Axon density was calculated by dividing axon count by optic nerve cross-sectional area.

3.9 Optic Nerve Grading

Cross sections of whole intact optic nerves were also assessed for damage using a semi-quantitative approach developed in the lab of John Morrison [35]. Six graders were trained to distinguish healthy from degenerating axons. Optic nerves were assigned a grade of 1 to 5, based upon combined analysis of low-magnification and high-magnification images of nerve cross sections. Grade 1 corresponds to healthy (naïve) appearance, while Grade 5 corresponds to heavily damaged appearance (few intact, healthy axons). Grades between these extremes correspond to intermediate degrees of damage. All scoring was conducted in a masked fashion.

3.10 Studies 4 and 5: Retinal Histology

Two groups of rats (n=3 each) were treated with either MB and light (Study 4) or with light alone (Study 5), allowed to recover, and euthanized 10 days later. Upon euthanasia, eyes were enucleated and placed in 2.5% glutaraldehyde solution for embedding, sectioning, and hematoxylin and eosin staining. Paraffin embedding was used for the group receiving MB and light, while cryosectioning was used for the group receiving light only. This difference in processing was the result of differing experimenter expertise.

3.11 Optical Coherence Tomography

Optical coherence tomography images (Bioptigen 4300, Leica Microsystems, Buffalo Grove, IL) were taken at 10 days post-injection in rats treated with light only. Anaesthesia was administered using ketamine/xylazine, and topical tetracaine (0.5%) and tropicamide (1%) were applied for local anaesthesia and dilation, respectively. A 3 mm radial scan (1,000 A-scans per B-scan), centered on the ONH, was collected for each eye. From the radial scan, B-scans oriented parallel to the anterior-posterior and nasal-temporal plane of the eye axes were assessed for evidence of treatment toxicity.

3.12 Statistical Analysis

Data are reported as mean ± standard deviation. Statistical analyses were performed using GraphPad Prism version 8.0.0 for Windows (GraphPad Software, San Diego, California). For the study of whole globe scleral mechanical properties, strain values were compared

using a two-way ANOVA (on the factors of experiment duration and scleral region) with matched pairs and adjusted for multiple comparisons using a Sidak correction. Axon counts and densities were analyzed with unpaired t-tests due to inability to analyze some samples. Nerve grade was analyzed with a paired Wilcoxon test. For electroretinograms, where multiple flash stimuli were employed, a two-way repeated measures ANOVA was used to compare effects across flash intensity and treatment. The F ratio statistic with numerator and denominator degrees of freedom (in parentheses) are reported, respectively. *Post hoc* tests were conducted with Sidak correction. The threshold for statistical significance was taken as $p=0.05$ for all tests.

4 Results

4.1 Confocal Imaging Study

Fluorescence due to MB was observed in and adjacent to the scleras of rats sacrificed at 10, 20, and 30 minutes after retrobulbar injection, with MB localization near, but not at, the ONH (Figure 2). Specifically, the average intensity (normalized to the largest value within each eye) was greatest at 1–2 mm from the ONH and decreased in both directions (towards and away from the ONH). Intensities near the ONH were low, likely due to the optic nerve itself blocking access of the MB to the sclera. Little difference was seen between 10, 20, and 30 min diffusion times. We conclude that MB was successfully delivered to the space immediately adjacent to the posterior sclera.

4.2 Scleral Stiffening in Rats Euthanized at Day 0 (Immediately After Treatment)

Having confirmed delivery of MB to the posterior sclera, we next used a whole globe inflation test (Figure 3A,B) to determine whether MB led to scleral stiffening. We determined average tissue strain at a pressure of 22 mmHg pressure in both the peripapillary (defined as the scleral region within a circle of diameter 2 mm centered on the optic nerve) and peripheral regions of MB + Light photocrosslinked and HBSS control scleras. Immediately after selective photocrosslinking, there was a significant decrease in strain, indicating an increase in stiffening, in the peripapillary region compared to the peripheral region of MB+Light photocrosslinked eyes ($1.20 \pm 0.47\%$ strain vs $2.22 \pm 0.73\%$ strain, respectively; n=7, p<0.05), corresponding to a 46% strain reduction (Figure 3C). Strain in the peripapillary sclera in the MB+Light photocrosslinked eyes also decreased compared to the peripapillary region of the HBSS contralateral control eye ($1.20 \pm 0.47\%$ strain vs $3.36 \pm 0.89\%$ strain, n=7, p<0.0001), corresponding to a 64% strain reduction. Together, these findings show that selective photocrosslinking with MB+Light significantly stiffened the peripapillary sclera compared to both the peripheral region of the same eye and the peripapillary region of HBSS contralateral control eyes.

Additional analysis showed that there was a statistically significant decrease in scleral strain in the peripheral region of the treated eye compared to that of the control eye ($2.67 \pm 0.71\%$ strain vs $3.32 \pm 1.32\%$ strain, n=7, p<0.05, respectively). This may be due to some off-target stiffening resulting from MB diffusion beyond the peripapillary region and light scattering in the peripheral region.

4.3 Scleral Stiffening in Rats Euthanized 6 Weeks After Treatment

To determine whether the scleral stiffening observed immediately after photocrosslinking persisted, we enucleated eyes from rats euthanized 6 weeks after treatment and determined scleral strains. Additional analyses were performed to assess differences in the ratios of strains (Figure S1). The scleral strain in the peripapillary region was significantly lower than in the peripheral region of photocrosslinked eyes ($1.42 \pm 0.29\%$ strain vs $2.67 \pm 0.71\%$ strain respectively, n=7, p<0.05), corresponding to a 47% strain reduction (Figure 3D). Peripapillary scleral strain in treated eyes was also lower than in the peripapillary region of HBSS contralateral control eyes ($1.42 \pm 0.29\%$ vs $3.20 \pm 0.95\%$ respectively, n=7, p<0.0001), corresponding to a 56% strain reduction. Moreover, comparison of strain in the peripapillary region of photocrosslinked eyes at Day 0 and Week 6 revealed no significant difference ($1.20 \pm 0.47\%$ vs $1.42 \pm 0.29\%$, n=7, p>0.05). These data show that selective stiffening of the peripapillary sclera persisted for at least 6 weeks after treatment and exceeded our target of 40% strain reduction.

4.4 Toxicity of Scleral Photocrosslinking in Rats Euthanized 6 Weeks After Treatment

Given the known toxicity of other sensitizers, we characterized the possible toxicity of MB photocrosslinking in the peripapillary sclera using optic nerve axon counts, axon densities, nerve grades, electroretinograms, and histology. Optic nerves collected from rats 6 weeks post-treatment indicated a deficit in RGC axon count (Figure 4) in photocrosslinked eyes ($46,500 \pm 11,100$ axons) compared to the HBSS-injected contralateral control eyes ($69,300 \pm 7,200$ axons, *p=0.0025*, unpaired t-test). A similar result was observed for axon density in photocrosslinked eyes ($203,000 \pm 42,000$ axons mm^{-2}) compared to HBSS-injected contralateral control eyes ($266,000 \pm 29,000$ axons mm^{-2}, *p=0.017*, unpaired t-test). Median nerve grade for photocrosslinked eyes (3.08 with 95% confidence interval of 2.71–3.96) was also markedly higher (indicating more severe damage) than that of HBSS controls (1.25 with 95% confidence interval of 1.10–1.57, *p=0.0078*, paired Wilcoxon test). Electroretinography revealed deficits in retinal response to a number of flash stimuli for light and dark-adapted conditions (Figure S2) including a-wave amplitude, b-wave amplitude, positive scotopic threshold response (pSTR) amplitude, photopic negative response (PhNR) amplitude, and flicker b-wave amplitude. See supplementary information for detailed electroretinography results.

4.5 Histology and OCT Imaging in Rats Exposed to MB and Light or Light Only

Toxicity of photocrosslinking was further assessed by examination of histological sections from rats euthanized 10 days after unilateral photocrosslinking treatment with MB and light to identify possible optic nerve and retinal damage. The contralateral naïve control eye was untreated (no injection or light). Sections were examined at the ONH and peripheral retina (>2 mm from the ONH) to assess retinal structure. Among the three rats in this study, one had evidence of inflammatory infiltration near the ON and retinal degradation adjacent to the ONH (Figure 5C, Figure S3C), the second rat appeared to have gliosis localized near the ONH (Figure S3E), and the third did not have any obvious damage to the optic nerve or retina (Figure S3G). Notably, all three rats had no damage in the peripheral retinas of the

treated eyes, indicating focal damage was likely caused by the presence of both MB and light near the peripapillary sclera (Figure 5D, Figure S3,D,F,H).

To assess possible damage from 660 nm light alone (without MB), another cohort of rats was treated according to the photocrosslinking procedure previously described with light only (no MB injection). Histological analysis did not reveal significant evidence of retinal damage in either the optic nerve region or the peripheral retina (Figure S4).

We also assessed possible effects of light exposure without MB by OCT (Figure S5). There were no apparent morphological differences between eyes exposed to targeted illumination compared to contralateral eyes receiving no treatment, further supporting findings from retinal histology indicating that 660 nm light alone used in this study did not cause any morphological damage to the retina.

5 Discussion

We have shown that selective peripapillary scleral crosslinking at the millimeter scale is possible *in vivo* and report a novel procedure for its implementation. Our approach used a photosensitizer, MB, administered by retrobulbar injection, followed by transpupillary illumination of the peripapillary region with 660nm red light. Importantly, this demonstrates that drug and light delivery challenges inherent in selectively crosslinking the posterior sclera may be overcome *in vivo*. This method is unique among existing ocular photocrosslinking protocols due to its spatial targeting of the peripapillary sclera. This method builds upon previous work in targeted scleral crosslinking, which was however limited to working with post mortem tissue or to the anatomically far more accessible equatorial sclera [7,37]. Our approach is novel due to its *in vivo* spatial targeting of the peripapillary sclera and the use of red light to better protect the retina.

We focused on strain as our outcome (as have most authors working in the glaucoma biomechanics field) because it is much easier to experimentally measure deformations (and hence deduce strains) than it is to measure local stresses in whole tissue. Of course, strains are intimately related to stresses through tissue mechanical properties, and it is thus not practical to conceptually decouple these quantities in complex systems such as the eye. Traditional photocrosslinking studies often report stiffness (Young's modulus) derived through uniaxial testing of segmented tissue samples. Measurement of strain in this study enabled quantification of mechanical properties in the intact posterior sclera which is more representative of the *in vivo* state.

The off-target scleral stiffening, i.e. in the peripheral sclera, that we observed at Day 0 may have been caused by light scattering within the posterior fundus tissues. Narrowing the beam size and reducing light intensity may further localize stiffening. For practical reasons, we chose in this study not to reduce the beam size since doing so would approach the lower bounds of spatial resolution on our globe inflation testing platform, which was used to assess scleral stiffness. Future studies may make use of atomic force microscopy to overcome this limitation. Additional *ex vivo* testing or tissue mechanics computational modeling is

warranted to understand the lower limits of beam size which would result in sufficient stiffening.

While light alone did not evidently alter the retinal or optic nerve head morphology, the photocrosslinking resulting from light exposure in the presence of MB had moderate adverse effects. This finding agrees with the literature on other singlet-oxygen generating photosensitizers which are known to have toxic effects when photoactivated *in vivo* [38–40]. Consistent with our targeted delivery approach, damage was isolated to the peripapillary region, as shown by histological analysis. Deficits seen in the electroretinography data may be related to damage from MB photoexcitation in the retina and in the optic nerve. Likewise, axon loss may have been caused by damage directly to the optic nerve or indirectly by collateral damage to axons in the retina that extend into the optic nerve.

While we attribute the observed toxicity to treatment photochemistry, we cannot definitively rule out stiffening as a contributor to retinal damage. One study showed that scleral stiffening, even in the equatorial region, was associated with damage away from the site of stiffening [37], although a second stiffening study did not find damage [8]. Furthermore, the optic nerve is known to undergo integrin-mediated changes in response to stiffening of the lamina cribrosa [41]. Integrin activation may lead to changes in astrocytes, Müller cells, or retinal blood vessels [41–44]. Therefore, changes to the mechanical microenvironment (such as local stiffening) may potentially contribute to retinal damage. More research in this area is needed.

Electroretinography revealed greater functional deficits at higher flash intensities (beyond the scotopic threshold) than at lower flash intensities. This observation may indicate selective damage of cone photoreceptors compared to rod photoreceptors, since cone function contributes to response at brighter flash intensities [45]. A possible explanation for selective cone damage is presence of a cone subpopulation with preferential absorbance for red light (red cones) compared to rods which have preferential absorbance in the blue-green wavelength range. However, rats generally lack sensitivity in the red wavelengths [46]. The damage to retinal function may also be due to non-specific photothermal damage in the strongly absorbing retinal pigment epithelium.

MB alone (without light) may play a role in the damage observed in the retina and optic nerve, as shown in prior studies that reported RGC toxicity in rats injected intravitreally with $2\ \mu L$ of MB at 2% (6.25 mM) concentration [42]. Comparatively, our $100\ \mu L$ retrobulbar injection at 3 mM represents a significantly higher dose, but our injection is separated from the retina by the sclera and choroid, which serve as a formidable clearance route and barrier to retinal entry. Thus, we expect that local MB concentrations in the retina were certainly lower than 3 mM in our study. The proximity of the optic nerve to the retrobulbar injection site may have caused the optic nerve to experience a high concentration of MB. Sensitizer biocompatibility is a subject of importance for any *in vivo* application, and in addition to the existing body of work for MB, future studies may be needed to assess effects on the specific tissues/concentrations in our study.

The light intensity used in this study (i.e., 424 mW/cm^2) exceeded the maximum permissible intensity for human eyes (211 mW/cm^2, calculated using ANSI 2000) exposed to 660 nm light for the given exposure conditions (see Supplemental information, Section 1.8) [48]. Considering the intensity used in this study exceeded the calculated maximum permissible intensity, it was unexpected that treatment with light alone caused no apparent changes in retinal morphology. We conclude that damage seen near the optic nerve due to the photocrosslinking procedure was not due to light alone and was likely a result of MB-mediated photochemistry. Though not assessed in this study, it is likewise possible that light of comparatively low intensity induced MB-mediated photochemistry in the periocular tissues where MB diffused from the retrobulbar injection site. These effects are expected to be minimal due to significant absorbance of light by the fundus tissue and MB within the sclera before reaching the periocular tissues.

Future clinical translation of peripapillary scleral stiffening as a treatment for glaucomatous optic neuropathy would need to balance the benefit of stiffening against any damage due to the stiffening procedure itself. The authors recognize that the present study is limited by virtue of having considered a single MB concentration and light intensity. We believe the observed toxicity could be most effectively reduced by lowering light intensity. While reducing light intensity may result in lower crosslink density, the scleral strain reductions that we measured in this study at 6 weeks post treatment (47% compared to peripheral sclera, 54% compared to contralateral peripapillary sclera) exceeded those reported by Coudrillier et al. (approximately 40%), which were shown to effectively reduce strain on the lamina cribrosa. Therefore, it may be possible to reduce light intensity and still induce sufficient crosslinking, but at less toxic levels. It has been reported by Wernli et al. that, for identical fluences of UVA illumination during riboflavin collagen crosslinking, higher light intensities result in less efficient crosslinking than lower light intensities [43,44]. The intensity of light reaching the sclera in our study was at the high end of the intensities used in the Wernli et al. study (~90 mW/cm^2), though direct comparison is difficult considering the different diffusion direction, sensitizer, and tissue studied.

Slowing MB diffusion to the optic nerve and retina could also reduce photocrosslinking toxicity. Formulation strategies may include MB conjugation to macromolecules or encapsulation in liposomes/carriers. Diffusion across the Tenon capsule at the posterior scleral surface may present a challenge. Its epithelialized surface is likely similar to that of the optic nerve sheath, making it difficult to design a delivery formulation capable of discriminating between the two. Alternatively, MB could be delivered by suprachoroidal injection, placing it at the interface of the sclera and choroid [51,52]. This approach is minimally invasive and overcomes any physical barriers to diffusion. However, only small volumes may be injected, and the choroid's adjacency would lead to rapid clearance.

A strategy to improve photocrosslinking efficiency may be to use a different sensitizer than MB. MB was chosen for its known low dark toxicity *in vivo*, efficient triplet yield, absorbance of red light in the phototherapeutic window, and its low cost/commercial availability. However, many other photosensitizers exist which may overcome limitations in this study due to their mechanisms of action, wavelengths of absorbance, and transport properties [45,46].

Besides potential application as a future glaucoma treatment, another interesting application for our targeted crosslinking approach is for treatment of myopia. Recently, the possibility of preventing myopic progression by scleral stiffening has attracted interest [57,58]. Targeted stiffening may be especially useful for correction of refractive error by differentially modulating scleral stiffness, resulting in controlled shaping of the eye. Both artificially produce regions of relatively stiffened sclera to control ocular deformation and hence produce a desired eye shape.

6   Conclusion

This study introduces a method for regionally targeted scleral photocrosslinking in the posterior globe using a novel microscope apparatus. We have shown MB and 660 nm red light to be efficacious at increasing scleral stiffness by as much as 54% compared to HBSS contralateral control eyes and by 47% compared to peripheral sclera in the same eye at 6 weeks post treatment. In its current form, this treatment generated moderate toxicity localized near the ONH; this toxicity affected retinal function, although effects on visual acuity remain to be assessed. Future studies should further optimize the procedure to reduce these adverse effects. Importantly, this study provides the means for future work to assess the impact of targeted peripapillary stiffening on functional and morphological outcomes in a glaucomatous animal model. Such a targeted approach to mechanical stabilization of the peripapillary region of the eye with reduced toxicity could provide a powerful new approach to glaucoma therapy that is mechanistically different from other approaches in use or under development today.

Supplementary Material

Refer to Web version on PubMed Central for supplementary material.

Acknowledgements

8   Data Availability

The raw/processed data required to reproduce these findings cannot be shared at this time due to technical or time limitations.

9   References

[1]. Tham Y-C, Li X, Wong TY, Quigley HA, Aung T, Cheng C-Y, Global Prevalence of Glaucoma and Projections of Glaucoma Burden through 2040: A Systematic Review and Meta-Analysis, Ophthalmology. 121 (2014) 2081–2090. 10.1016/j.ophtha.2014.05.013. [PubMed: 24974815]

[2]. Kingman S, Glaucoma is second leading cause of blindness globally., Bull. World Health Organ. 82 (2004) 887–888. https://www.scopus.com/inward/record.uri?eid=2-

s2.0-14544301551&partnerID=40&md5=12220dded577e176dd21ceef8f42b900. [PubMed: 15640929]

[3]. Russo R, Pasquale G, Adornetto A, Nucci C, Tiziana M, Bagetta G, Antonio L, Retinal ganglion cell death in glaucoma : Exploring the role of neuroin fl ammation, 787 (2016) 134–142. 10.1016/j.ejphar.2016.03.064.

[4]. Cheema A, Chang RT, Shrivastava A, Singh K, Update on the Medical Treatment of Primary Open-Angle Glaucoma, 5 (2016) 51–58. 10.1097/APO.0000000000000181.

[5]. Strouthidis NG, Girard MJA, Altering the way the optic nerve head responds to intraocular pressure—a potential approach to glaucoma therapy, Curr. Opin. Pharmacol 13 (2013) 83–89. . [PubMed: 22999652]

[6]. Coudrillier B, Campbell IC, Read AT, Geraldes DM, Vo NT, Feola A, Mulvihill J, Albon J, Abel RL, Ethier CR, Effects of peripapillary scleral stiffening on the deformation of the lamina cribrosa, Investig. Ophthalmol. Vis. Sci 57 (2016) 2666–2677. 10.1167/iovs.15-18193. [PubMed: 27183053]

[7]. Thornton IL, Dupps WJ, Roy AS, Krueger RR, Biomechanical effects of intraocular pressure elevation on optic nerve/lamina cribrosa before and after peripapillary scleral collagen cross-linking, Investig. Ophthalmol. Vis. Sci 50 (2009) 1227–1233. 10.1167/iovs.08-1960. [PubMed: 18952911]

[8]. Kimball EC, Nguyen C, Steinhart MR, Nguyen TD, Pease ME, Oglesby EN, Oveson BC, Quigley HA, Experimental scleral cross-linking increases glaucoma damage in a mouse model, Exp. Eye Res 128 (2014) 129–140. . [PubMed: 25285424]

[9]. Clayson K, Pan X, Pavlatos E, Short R, Morris H, Hart RT, Liu J, Corneoscleral stiffening increases IOP spike magnitudes during rapid microvolumetric change in the eye, Exp. Eye Res 165 (2017) 29–34. . [PubMed: 28864177]

[10]. Wollensak G, Spoerl E, Seiler T, Riboflavin/ultraviolet-a–induced collagen crosslinking for the treatment of keratoconus, Am. J. Ophthalmol 135 (2003) 620–627. . [PubMed: 12719068]

[11]. Raiskup F, Theuring A, Pillunat LE, Corneal collagen crosslinking with riboflavin and ultraviolet-A light in progressive keratoconus : Ten-year results, J. Cart. Refract. Surg 41 (2015) 41–46. 10.1016/j.jcrs.2014.09.033.

[12]. Wollensak G, Iomdina E, Long-term biomechanical properties of rabbit sclera after collagen crosslinking using riboflavin and ultraviolet A (UVA), Acta Ophthalmol 87 (2009) 193–198. 10.1111/j.1755-3768.2008.01229.x. [PubMed: 18803623]

[13]. Wollensak G, Spoerl E, Collagen crosslinking of human and porcine sclera, (2004). 10.1016/j.jcrs.2003.11.032.

[14]. Wollensak G, Iomdina E, Dittert D-D, Salamatina O, Stoltenburg G, Cross-linking of scleral collagen in the rabbit using riboflavin and UVA, Acta Ophthalmol. Scand 83 (2005) 477–482. 10.1111/j.1600-0420.2005.00447.x. [PubMed: 16029274]

[15]. Wang M, Zhang F, Qian X, Zhao X, Regional Biomechanical Properties of Human Sclera After Cross-linking by Riboflavin/Ultraviolet A, J. Refract. Surg 28 (2012) 723–728. 10.3928/1081597X-20120921-08. [PubMed: 23062003]

[16]. Kwok SJJ, Forward S, Wertheimer CM, Liapis AC, Lin HH, Kim M, Seiler TG, Birngruber R, Kochevar IE, Seiler T, Yun S-H, Selective Equatorial Sclera Crosslinking in the Orbit Using a Metal-Coated Polymer Waveguide, Invest. Ophthalmol. Vis. Sci 60 (2019) 2563–2570. 10.1167/iovs.19-26709. [PubMed: 31212308]

[17]. Avila MY, Gerena VA, Navia JL, Corneal crosslinking with genipin, comparison with UV-riboflavin in ex-vivo model, Mol. Vis 18 (2012) 1068–1073. https://www.ncbi.nlm.nih.gov/pubmed/22605919. [PubMed: 22605919]

[18]. Liu TX, Wang Z, Collagen crosslinking of porcine sclera using genipin, Acta Ophthalmol 91 (2013) 253–257. 10.1111/aos.12172.

[19]. Hannon BG, Schwaner SA, Boazak EM, Gerberich BG, Winger EJ, Prausnitz MR, Ethier CR, Sustained scleral stiffening in rats after a single genipin treatment, J. R. Soc. Interface. 16 (2019) 20190427. 10.1098/rsif.2019.0427. [PubMed: 31615330]

[20]. Schirmer RH, Adler H, Pickhardt M, Mandelkow E, "Lest we forget you — methylene blue …," Neurobiol. Aging. 32 (2011) 2325.e7–2325.e16. .

[21]. Orth K, Beck G, Genze F, Rück A, Methylene blue mediated photodynamic therapy in experimental colorectal tumors in mice, J. Photochem. Photobiol. B Biol 57 (2000) 186–192. .

[22]. Ken Gillman P, Review: CNS toxicity involving methylene blue: The exemplar for understanding and predicting drug interactions that precipitate serotonin toxicity, J. Psychopharmacol 25 (2011) 429–436. 10.1177/0269881109359098. [PubMed: 20142303]

[23]. Rice L, Wainwright M, Phoenix DA, Wainwright M, Photosensitizers DAPP, Phenothiazine Photosensitizers. III. Activity of Methylene Blue Derivatives against Pigmented Melanoma Cell Lines Activity of Methylene Blue Derivatives against, 9478 (2013).

[24]. WENDEL WB, METHYLENE BLUE, METHEMOGLOBIN, AND CYANIDE POISONING, J. Pharmacol. Exp. Ther 54 (1935) 283 LP–298. http://jpet.aspetjournals.org/content/54/3/283.abstract.

[25]. Fernández-Pérez A, Valdés-Solís T, Marbán G, Visible light spectroscopic analysis of Methylene Blue in water; the resonance virtual equilibrium hypothesis, Dye. Pigment 161 (2019) 448–456. 10.1016/j.dyepig.2018.09.083.

[26]. Alarcón E, Edwards AM, Aspee A, Moran FE, Borsarelli CD, Lissi EA, Gonzalez-Nilo D, Poblete H, Scaiano JC, Photophysics and photochemistry of dyes bound to human serum albumin are determined by the dye localization, Photochem. Photobiol. Sci 9 (2010) 93–102. 10.1039/b9pp00091g. [PubMed: 20062849]

[27]. D browski JM, Arnaut LG, Photodynamic therapy (PDT) of cancer: From local to systemic treatment, Photochem. Photobiol. Sci 14 (2015) 1765–1780. 10.1039/c5pp00132c. [PubMed: 26219737]

[28]. Sionkowska A, The influence of methylene blue on the photochemical stability of collagen, Polym. Degrad. Stab 67 (2000) 79–83. .

[29]. Ramshaw JAM, Stephens LJ, Tulloch PA, Biochi~ic~a et Biophysica A~ta, 1206 (1994) 225–230.

[30]. Kozma EM, Wisowski G, Jura-Poltorak A, Olczyk P, Olczyk K, Nawrat Z, The influence of physical and chemical agents on photooxidation of porcine pericardial collagen., Biomed. Mater. Eng 15 (2005) 137–144. [PubMed: 15911995]

[31]. Chisholm JM, Pang DSJ, Assessment of Carbon Dioxide, Carbon Dioxide/Oxygen, Isoflurane and Pentobarbital Killing Methods in Adult Female Sprague-Dawley Rats., PLoS One. 11 (2016) e0162639. 10.1371/journal.pone.0162639. [PubMed: 27648836]

[32]. Valentine H, Williams WO, Maurer KJ, Sedation or inhalant anesthesia before euthanasia with CO2 does not reduce behavioral or physiologic signs of pain and stress in mice., J. Am. Assoc. Lab. Anim. Sci 51 (2012) 50–57. [PubMed: 22330868]

[33]. Campbell IC, Hannon BG, Read AT, Sherwood JM, Schwaner SA, Ethier CR, Quantification of the efficacy of collagen cross-linking agents to induce stiffening of rat sclera, J R Soc Interface. 14 (2017). 10.1098/rsif.2017.0014.

[34]. Mihai LA, Chin L, Janmey PA, Goriely A, A comparison of hyperelastic constitutive models applicable to brain and fat tissues, J. R. Soc. Interface. 12 (2015) 486. 10.1098/rsif.2015.0486.

[35]. Jia L, Cepurna WO, Johnson EC, Morrison JC, Patterns of intraocular pressure elevation after aqueous humor outflow obstruction in rats, Invest. Ophthalmol. Vis. Sci 41 (2000) 1380–1385. [PubMed: 10798653]

[36]. Ritch MD, Hannon BG, Read AT, Feola AJ, Cull GA, Reynaud J, Morrison JC, Burgoyne CF, Pardue MT, Ethier CR, AxoNet: A deep learning-based tool to count retinal ganglion cell axons., Sci. Rep 10 (2020) 8034. 10.1038/s41598-020-64898-1. [PubMed: 32415269]

[37]. Li Y, Zhang F, Sun M, Lai L, Lv X, Liu C, Wang M, Wang N, Safety and long-term scleral biomechanical stability of rhesus eyes after scleral cross-linking by blue light, Curr. Eye Res (2020) null–null. 10.1080/02713683.2020.1853781.

[38]. Banfi S, Caruso E, Caprioli S, Mazzagatti L, Canti G, Ravizza R, Gariboldi M, Monti E, Photodynamic effects of porphyrin and chlorin photosensitizers in human colon adenocarcinoma cells, Bioorg. Med. Chem 12 (2004) 4853–4860. . [PubMed: 15336264]

[39]. Bäumler W, Abels C, Karrer S, Weiß T, Messmann H, Landthaler M, Szeimies R-M, Photo-oxidative killing of human colonic cancer cells using indocyanine green and infrared light, Br. J. Cancer. 80 (1999) 360–363. 10.1038/sj.bjc.6690363. [PubMed: 10408838]

[40]. Xiao L, Gu L, Howell SB, Sailor MJ, Porous Silicon Nanoparticle Photosensitizers for Singlet Oxygen and Their Phototoxicity against Cancer Cells, ACS Nano. 5 (2011) 3651–3659. 10.1021/nn1035262. [PubMed: 21452822]

[41]. Morrison JC, Integrins in the optic nerve head: potential roles in glaucomatous optic neuropathy (an American Ophthalmological Society thesis), Trans. Am. Ophthalmol. Soc 104 (2006) 453–477. https://pubmed.ncbi.nlm.nih.gov/17471356. [PubMed: 17471356]

[42]. Tawil NJ, Wilson P, Carbonetto S, Expression and distribution of functional integrins in rat CNS glia., J. Neurosci. Res 39 (1994) 436–447. 10.1002/jnr.490390411. [PubMed: 7533845]

[43]. Guidry C, Bradley KM, King JL, Tractional force generation by human muller cells: growth factor responsiveness and integrin receptor involvement, Invest. Ophthalmol. Vis. Sci 44 (2003) 1355–1363. [PubMed: 12601069]

[44]. Brem RB, Robbins SG, Wilson DJ, O'Rourke LM, Mixon RN, Robertson JE, Planck SR, Rosenbaum JT, Immunolocalization of integrins in the human retina., Invest. Ophthalmol. Vis. Sci 35 (1994) 3466–3474. [PubMed: 8056522]

[45]. Green DG, Scotopic and photopic components of the rat electroetinogram, J. Physiol 228 (1973) 781–797. 10.1113/jphysiol.1973.sp010112. [PubMed: 4702156]

[46]. Lamb TD, Photoreceptor spectral sensitivities: Common shape in the long-wavelength region, Vision Res 35 (1995) 3083–3091. . [PubMed: 8533344]

[47]. Fiedorowicz M, Schuettauf F, Haritoglu C, May CA, Messias A, Kampik A, Choragiewicz TJ, Schatz A, Thaler S, Zrenner E, in Vivo Toxicity Testing of Methyl Blue and Aniline Blue As Vital Dyes for Intraocular Surgery, Retina. 29 (2009) 1257–1265. 10.1097/iae.0b013e3181b8615b. [PubMed: 19934820]

[48]. Delori FC, Webb RH, Sliney DH, Maximum permissible exposures for ocular safety (ANSI 2000), with emphasis on ophthalmic devices, J. Opt. Soc. Am. A 24 (2007) 1250. 10.1364/josaa.24.001250.

[49]. Wernli J, Schumacher S, Spoerl E, Mrochen M, The efficacy of corneal cross-linking shows a sudden decrease with very high intensity UV light and short treatment time, Investig. Ophthalmol. Vis. Sci 54 (2013) 1176–1180. 10.1167/iovs.12-11409. [PubMed: 23299484]

[50]. Hammer A, Richoz O, Mosquera SA, Tabibian D, Hoogewoud F, Hafezi F, Corneal biomechanical properties at different corneal cross-linking (CXL) irradiances, Investig. Ophthalmol. Vis. Sci 55 (2014) 2881–2884. 10.1167/iovs.13-13748. [PubMed: 24677109]

[51]. Jung JH, Desit P, Prausnitz MR, Targeted Drug Delivery in the Suprachoroidal Space by Swollen Hydrogel Pushing, Invest. Ophthalmol. Vis. Sci 59 (2018) 2069–2079. 10.1167/iovs.17-23758. [PubMed: 29677369]

[52]. Jung JH, Park S, Chae JJ, Prausnitz MR, Collagenase injection into the suprachoroidal space of the eye to expand drug delivery coverage and increase posterior drug targeting, Exp. Eye Res 189 (2019) 107824. [PubMed: 31585119]

[53]. Mellish KJ, Brown SB, Verteporfin: a milestone in opthalmology and photodynamic therapy, Expert Opin. Pharmacother 2 (2001) 351–361. 10.1517/14656566.2.2.351. [PubMed: 11336591]

[54]. Brandis A, Mazor O, Neumark E, Rosenbach-Belkin V, Salomon Y, Scherz A, Novel Water-soluble Bacteriochlorophyll Derivatives for Vascular-targeted Photodynamic Therapy: Synthesis, Solubility, Phototoxicity and the Effect of Serum Proteins¶, Photochem. Photobiol 81 (2005) 983. 10.1562/2004-12-01-ra-389r1.1. [PubMed: 15839743]

[55]. Gawargious BA, Le A, Lesgart M, Ugardar S, Demer JL, Differential Regional Stiffening of Sclera by Collagen Cross-linking, Curr. Eye Res (2019) 1–8.

[56]. Li Y, Liu C, Sun M, Lv X, Wang M, Jiao X, Zhang L, Wang N, Zhang F, Ocular safety evaluation of blue light scleral cross-linking in vivo in rhesus macaques, Graefe's Arch. Clin. Exp. Ophthalmol 257 (2019) 1435–1442. [PubMed: 31065848]

[57]. Grytz R, Siegwart JT, Changing material properties of the tree shrew sclera during minus lens compensation and recovery, Invest. Ophthalmol. Vis. Sci 56 (2015) 2065–2078. [PubMed: 25736788]

[58]. Wang M, Yang Z-K, Liu H, Li R, Liu Y, Zhong W-J, Genipin inhibits the scleral expression of miR-29 and MMP2 and promotes COL1A1 expression in myopic eyes of guinea pigs, Graefe's Arch. Clin. Exp. Ophthalmol (2020) 1–8.

Highlights:

1. Localized stiffening of the posterior eye may be a treatment strategy for glaucoma and myopia

2. We sought to photocrosslink scleral collagen, using methylene blue as a photoinitiator, *in vivo*

3. We stiffened an annular region around the optic nerve with a transpupillary red light beam

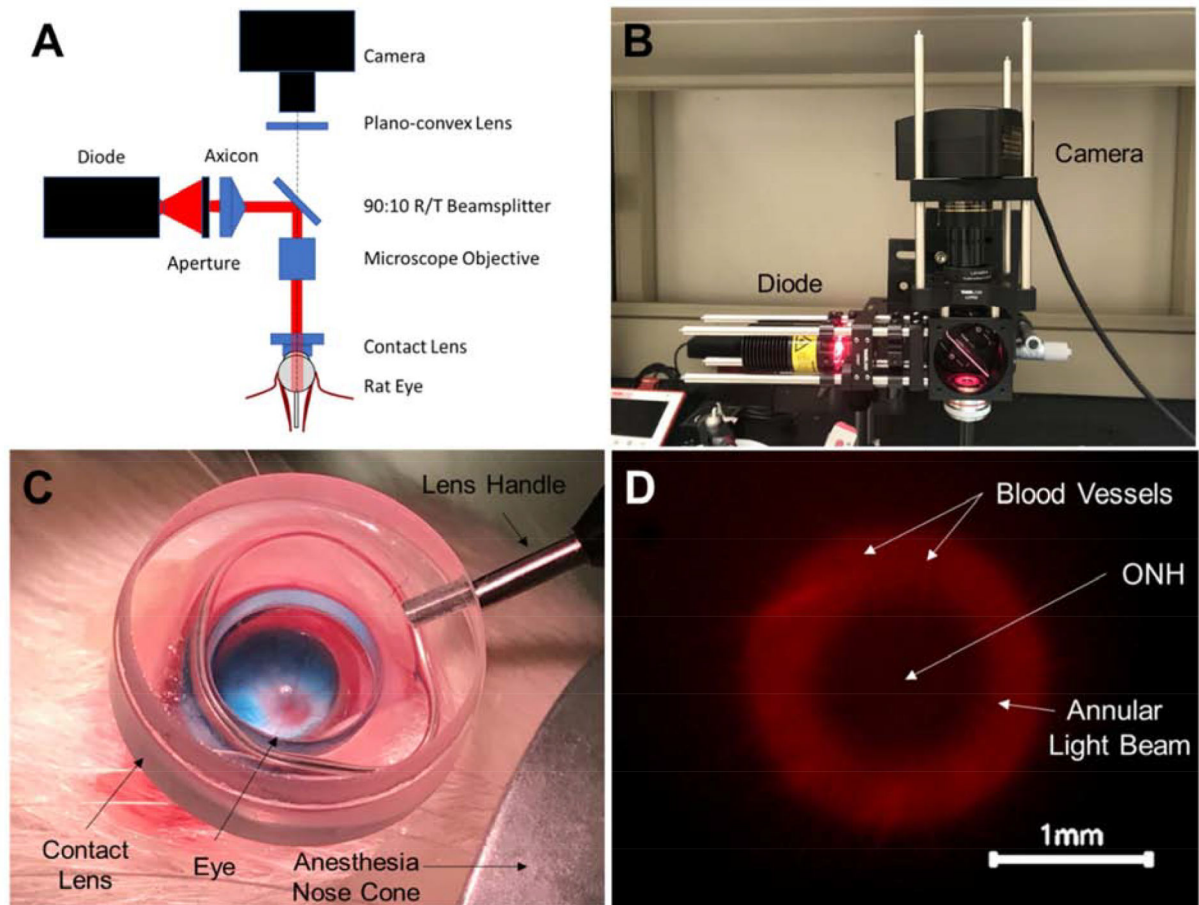4. Moderate treatment toxicity was identified using axon counts, histology, and electroretinography

Figure 1:
Ophthalmic microscope designed to enable simultaneous transpupillary fundus visualization and annular beam projection in the rat eye *in vivo*. A) Component diagram, and B) photographic image of the microscope. The microscope allowed a user to simultaneously project an annular beam onto a rat fundus, observe the location of the beam on the fundus, and precisely position the beam using a three-axis manual micro-positioner stage (behind the microscope). C) A contact lens placed on the corneal surface created a clear visual path for viewing the rat fundus. The optic disc can be seen (red disc) from which blood vessels emanate. The blue color is due to the retrobulbar injection of MB, visible in this case in a non-pigmented Wistar rat. D) Image from microscope camera during illumination procedure in a Brown Norway rat (pigmented) showing annular beam spot relative to the ONH (center). The beam illumination is shown in red, with black indicating non-illuminated regions.
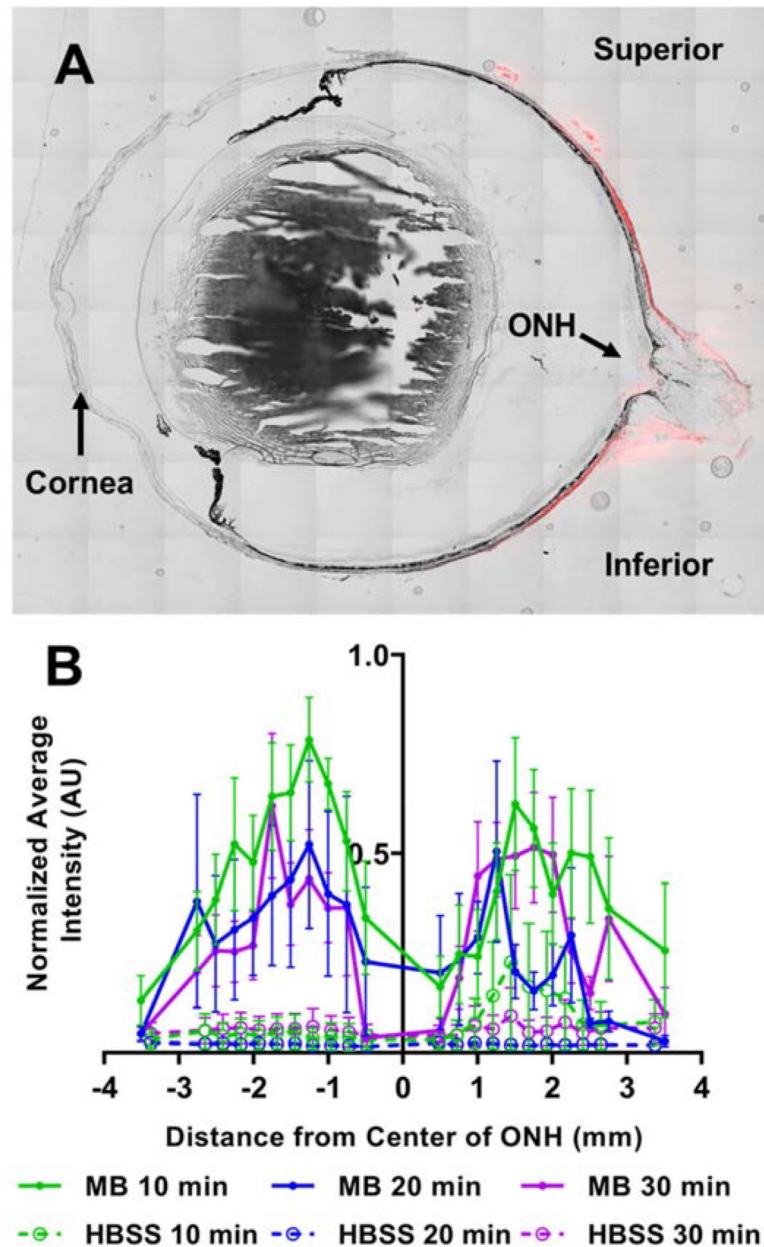
Figure 2:
Fluorescence intensity of MB in sclera of rats. A) Representative section through an eye showing red fluorescence distribution due to MB at the posterior globe near the optic nerve head (ONH). B) Relative fluorescence intensity of MB in rats euthanized 10 (n=5), 20 (n=3), or 30 (n=5) min after injection. Experimental animals received MB injection. Control animals received sham injection of HBSS. Average intensity was first calculated at specific distances from the ONH. The average intensity at each distance was then normalized by the greatest average intensity value in each animal. Negative and positive x-axis values indicate distance in the inferior and superior direction from the ONH, respectively. Symbols show mean ± standard error of the mean (SEM).
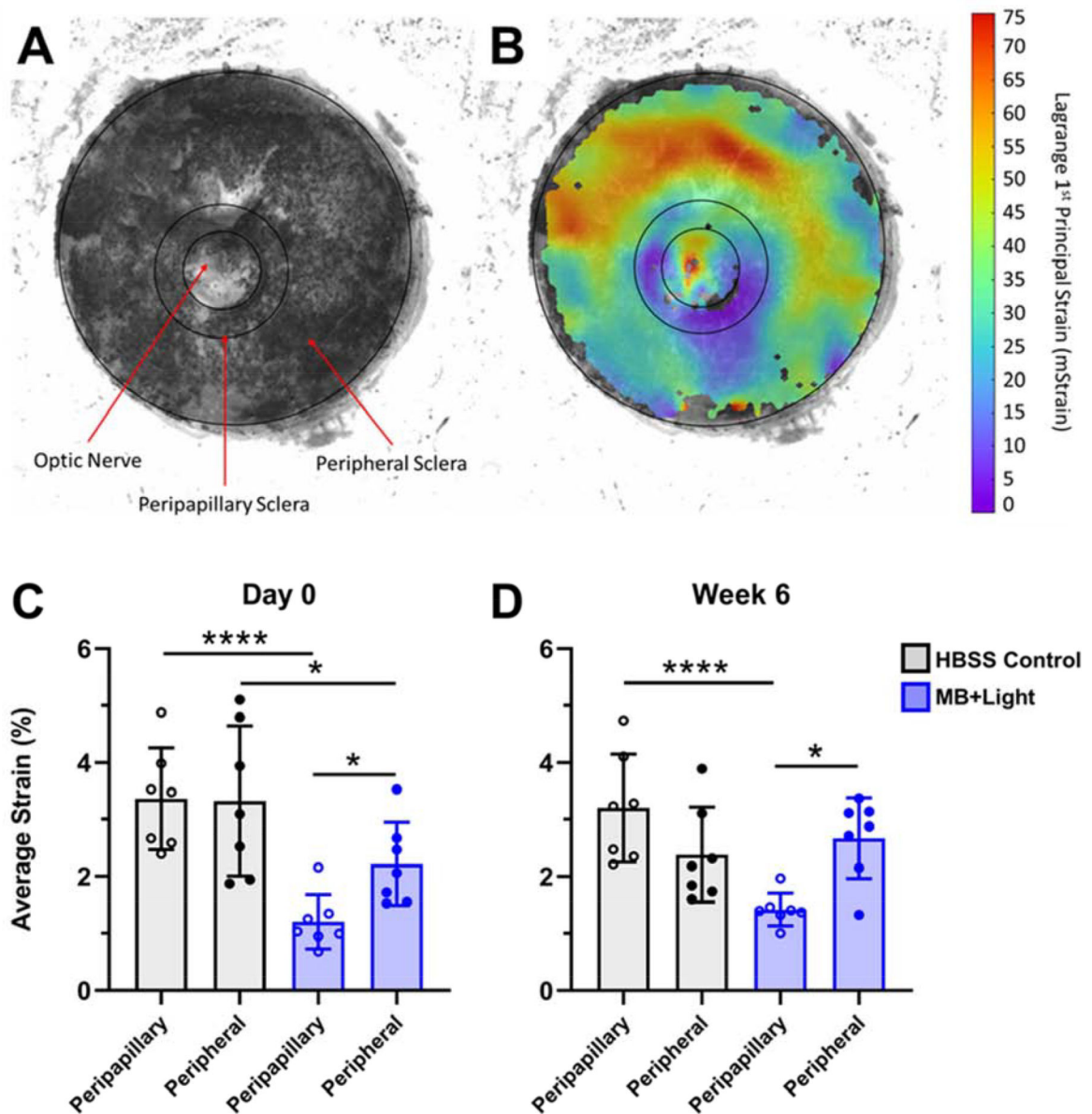
Figure 3:
Whole globe inflation testing was used to determine the spatial distribution of strain values on the posterior, external scleral surface. A) The position of graphite microparticles was tracked on the scleral surface as a function of applied intraocular pressure. B) Digital image correlation analysis generated spatial strain maps, from which average strain was calculated. Strain values were determined across the peripapillary scleral region and the peripheral scleral region (labeled in A) separately. Values were reported for both HBSS contralateral control eyes and photocrosslinking-treated eyes, resulting in four values per animal. Average strain is plotted at a pressure of 22 mmHg in peripapillary and peripheral regions of the posterior rat eye at C) Day 0, or D) Week 6 post-photocrosslinking treatment. Experimental eyes received selective photocrosslinking of the peripapillary region, whereas control eyes were HBSS-injected contralateral eyes. Bars show mean ± standard deviation from n=7

replicates per data point. Note, strain values are reported in this study as % strain, converted from the units of mStrain represented in panel B. * p<0.05. **** p<0.0001.
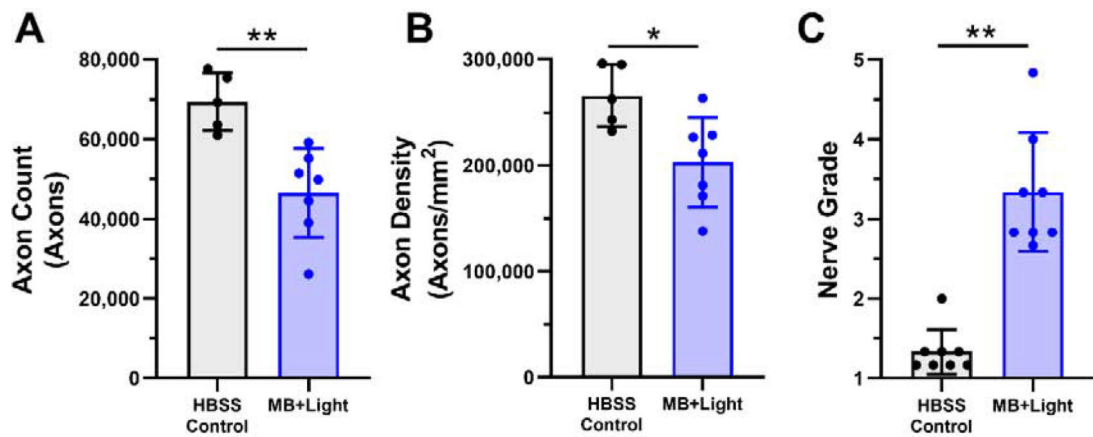
Figure 4:
A) Optic nerve axon counts, B) optic nerve axon densities (axon count normalized by nerve cross-sectional area), and C) nerve grades of rats 6 weeks after treatment with MB photocrosslinking (MB+Light). Control eyes were injected with HBSS and did not receive MB or light. Data points show mean ± standard deviation. For axon count and nerve density, n=5 for HBSS control and n=7 for MB+light due to limitations of axon counting software ability to analyze some sections. For nerve grade, n=8 for both HBSS control and MB +Light. * p<0.05, ** p<0.01, *** p<0.001.
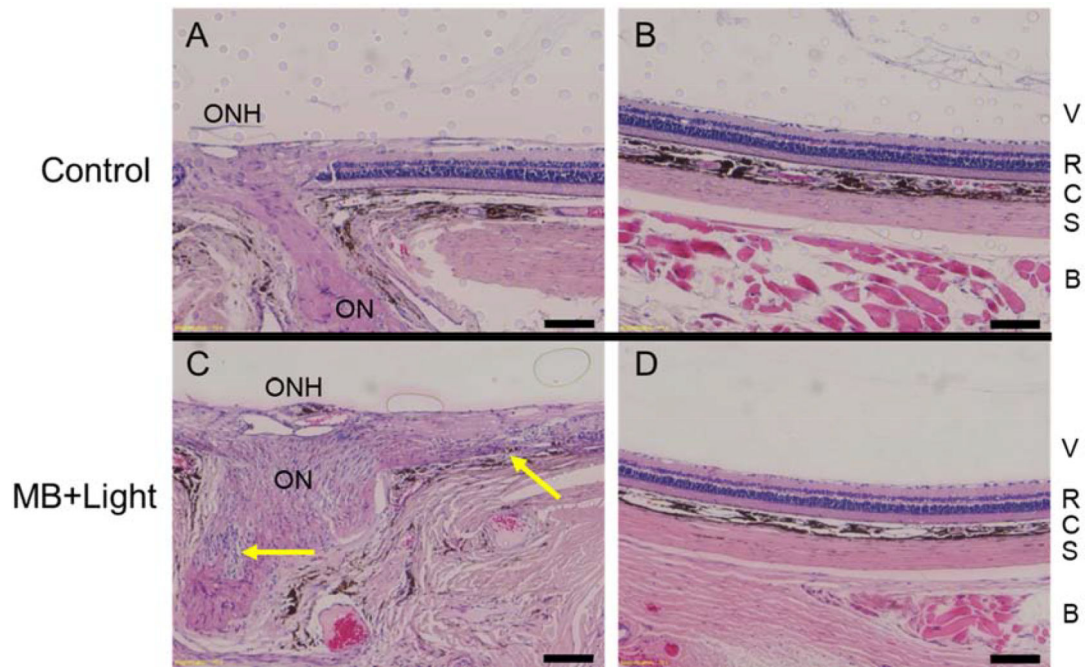
Figure 5:
Histological sections of optic nerve head (ONH) and peripheral retina (> 2 mm from ONH) from rats euthanized 10 days after unilateral treatment with targeted MB photocrosslinking were used to assess safety after photocrosslinking. Paraffin-embedded sections were stained with hematoxylin and eosin. While local tissue responses varied in eyes after photocrosslinking, we show the most severe damage seen among the three treated eyes from 3 rats examined. Control eye (retrobulbar injection of HBSS) showing healthy optic nerve and healthy retina both A) adjacent to the ONH, and B) in the periphery. C) A treated eye shows inflammatory infiltration near the ON (lower arrow) and retinal damage (upper arrow) near the ON. This damage was localized to the region adjacent to the optic nerve, since retina in the D) periphery appeared normal. Abbreviations: optic nerve head (ONH), optic nerve (ON), vitreous (V), retina (R), choroid (C), sclera (S), and retrobulbar tissue (B). Scale bars = 100 μm.

Table 1:

Summary of individual studies and outcome measures.

Study	Sample Size, Study Duration	Treatment, Primary Eye	Treatment, Contralateral Eye	Analysis
Confocal Microscopy/MB Distribution	n=13 total BN rats, euthanized at: 10 mins post injection (n=5), 20 mins post injection (n=3), 30 mins post injection (n=5)	30 mM MB (5O ul, retrobulbar)	HBSS (50 ul, retrobulbar)	**Confocal microscopy:** MB transport to sclera
Scleral Stiffening in Rats Euthanized at Day 0 (Immediately After Treatment)	n=7 BN rats, euthanized immediately post treatment	3 mM MB (100 ul retrobulbar), illumination [*]	HBSS (100 ul, retrobulbar)	**Whole globe inflation:** scleral strain
Scleral Stiffening in Rats Euthanized 6 Weeks After Treatment	n=8 BN rats, euthanized 6 weeks post treatment	3 mM MB (100 ul retrobulbar), illumination [*]	HBSS (100 ul, retrobulbar)	**Whole globe inflation:** scleral strain **Electroretinography:** retinal function **Axon Count/Grade:** ON/retinal health
Histology (MB+light)	n=3 BN rats, euthanized 10 days post treatment	3 mM MB (100 ul retrobulbar), illumination [*]	N/A [**]	**Histology:** ON/retinal morphology
Histology (Light Only)	n=3 BN rats, euthanized 10 days post treatment	Illumination [*]	N/A [**]	**Histology:** ON/retinal morphology **OCT:** retinal morphology

Abbreviations: MB (methylene blue), BN (Brown Norway), HBSS (Hank's Balanced Salt Solution), ON (Optic Nerve), OCT (Optical Coherence Tomography),

[*] Illumination was performed using a 30 minute transpupillary exposure of the peripapillary sclera to 424 m W/cm2 660 nm light.

[**] Naive (untreated) controls.